IEEE Access
Multidisciplinary | Rapid Review | Open Access Journal

Received December 24, 2020, accepted January 12, 2021, date of publication January 18, 2021, date of current version February 5, 2021.

Digital Object Identifier 10.1109/ACCESS.2021.3052185

A SVD-Based Signal De-Noising Method With Fitting Threshold for EMAT

BITING LEI, PENGXING YI, (Member, IEEE), JIAYUN XIANG, AND WEI XU
School of Mechanical Science and Engineering, Huazhong University of Science and Technology, Wuhan 430074, China

Corresponding author: Pengxing Yi (pxyi@hust.edu.cn)

This work was supported by the National Key Research and Development Program under Grant 2018YFB2003303.

ABSTRACT The electromagnetic acoustic transducer (EMAT) is a powerful and useful non-destructive testing technology for structural health monitoring. However, EMAT has an issue of low efficiency in conversion and its signal is easily affected by noise, which make it difficult to accurately identify and evaluate structural defects. Thereby, signal de-noising preprocessing is essential for the evaluation of defects. In this paper, we proposed an improved singular value decomposition (SVD) de-noising method based on the fitting threshold for EMAT signal. For SVD de-noising method, the key point is to determine the singular value threshold for reconstructing the signal. We applied a segmented regression model to find the appropriate threshold in this approach. To investigate the efficacy of the proposed method, simulation signals and experimental signals are used for verification respectively. A comparative analysis has been under-taken to confirm that the proposed signal de-noising has advantages over other methods in EMAT signal noise reduction, and it is useful for more accurate evaluation of defects.

INDEX TERMS De-noising, electromagnetic acoustic transducer, fitting threshold, SVD.

I. INTRODUCTION

Surface defect identification and evaluation is an important part of structural health monitoring. At present, various non-destructive testing methods, such as ultrasonic testing, eddy current testing, magnetic memory testing, are applied to identify and evaluate surface defects due to different environments [1]–[3]. Among these popular methods, electromagnetic acoustic transducer (EMAT) is widely used for the advantages of high precision, no coupling agent, non-contact and flexible detection [4]–[6]. Rayleigh wave-based electromagnetic ultrasound is often used to detect and evaluate surface defects due to its energy concentration on the surface. The EMAT signal is a non-stationary signal, which is weak and vulnerable to noise and external electromagnetic interference [7], [8]. The characteristic values of evaluation defects are submerged in noise and cannot be extracted accurately. Therefore, a suitable and effective de-noising method for the EMAT signal is very important for the quantitative evaluation of defects. A noise reduction method suitable for EMAT signals must meet certain requirements. Especially, the key features of the signal should not change as a result of de-noising.

Many efforts have been made to reduce noise in the EMAT signal. Wavelet de-noising, SVD de-noising algorithm, and empirical mode decomposition (EMD) de-noising algorithm are some of techniques proposed to preprocess signals [7], [9], [10]. These methods may work well under certain circumstances but they may not be optimal for EMAT signal. The wavelet de-noising method has no obvious effect on weak signals and signals with less signal-to-noise ratio [11]–[13]. Additionally, wavelet de-noising is limited by the choice of wavelet threshold function, decomposition level, and wavelet basis function. EMD has non-negligible end-point effects and modal aliasing. So, we need to find a noise reduction method that is effective for EMAT signals.

The singular value decomposition method attracts researchers' attention for its less phase shift and no delay and it is sensitive to weak signals in noise. SVD can be widely used in many fields. Wen *et al.* [7], Li *et al.* [14] applied SVD to inspect the health conditions of important components and diagnose faults. The SVD method can also be used to extract features [8], [15]. In addition, SVD de-noising method can be used to improve the signal-to-noise ratio of signals [16], [17], and which can meet certain requirements of EMAT signals noise reduction. As far as we know, the information of signal is reflected in the sequence of singular values, so the key point of SVD noise reduction method is how to determine the effective order of singular values for the reconstructed signal. The traditional determination methods of reconstructed order include the fixed threshold method [18], singular entropy increment [17], singular value curvature spectrum [8], and

The associate editor coordinating the review of this manuscript and approving it for publication was Xiaojie Su.

singular value difference spectrum [19]. Yang *et al.* [18] used a fixed threshold truncation method in the process of processing signals with SVD to significantly improve the performance of a three-axis magnetometer (TAM). For different signals, the singular value de-noising method based on a fixed threshold has no universality, and the selection of fixed threshold has a great influence on noise reduction. Singular value difference spectrum and singular value curvature spectrum cannot always effectively determine the reconstruction order and lose useful signals [8], [19]. Singular value entropy sequences have no obvious characteristics for determining the number of effective singular values. Thereby, a suitable selection method of the effective order of singular values is very important for SVD noise reduction, which is also the main of this paper.

Since the singular values of EMAT signals are abrupt and the difference of singular value in magnitude between main signal and noise is obvious, we make effort to find a threshold that can be used to distinguish the singular value of the noise and the main signal to achieve the purpose of noise reduction. According to the characteristics of the singular value sequence, the slope change point is the boundary point of the singular value between the noise and the main signal. However, neither the maximum value of the singular value difference spectrum nor the maximum value of the singular value curvature can accurately determine the position of the slope change point. In order to find the slope change point, we propose a fitting threshold method based on segmented regression in this paper. Firstly, the singular value sequence is equally divided into several segments, and then the second-order difference spectrum of each segment is obtained separately. Finally, the number of effective singular values is determined by the intersection point of the fitting curves in the adjacent interval of the second-order difference spectrum maximum value. The major contribution of this paper: we propose a fitting threshold determination method based on segmented regression method for improving the SVD de-noising method, and verify that the proposed method is suitable for EMAT signal noise reduction.

The rest of this paper is organized as follows. In Section II, the principle of the SVD and the threshold determination method are described. Section III verifies the effectiveness of the proposed method using simulated signals. The comparison results of different noise reduction methods and characterization results are analyzed in Section IV. Section V presents the conclusions.

II. SVD-BASED SIGNAL PROCESSING METHOD

For electromagnetic acoustic testing, it is of prime importance to extract the feature of the transmitted signal for identifying and evaluating the defect. However, the signals of EMAT are easily affected by noise for its physical mechanism. The important information of the received signal will be buried in noise. In order to keep important information of signals, we introduce an improved singular value decomposition method for EMAT signal noise reduction.

A. SINGULAR VALUE DECOMPOSITION

We first take a brief review of SVD. Assuming that the received signal from EMAT is $\mathrm{X} = (\mathrm{x}\,(1)\,, \mathrm{x}\,(2)\,, \cdots, \mathrm{x}\,(\mathrm{N}))$. It is necessary to reshape the signal $\boldsymbol{X}$ into a matrix for SVD. Here, we chose the Hankel matrix to obtain the matrix due to its zero phase shift property and wavelet-like characteristics [7]. The Hankel matrix of the signal $\boldsymbol{X}$ is:

$$H = \begin{bmatrix} x\,(1) & x\,(2) & \cdots & x\,(\mathrm{n}) \\ x\,(2) & x\,(3) & \cdots & x\,(n+1) \\ \vdots & \vdots & \vdots & \vdots \\ x\,(m) & x\,(m+1) & \cdots & x\,(N) \end{bmatrix} \tag{1}$$

If the number of columns is closer to the number of rows, that is, the constructed Hankel matrix is square or close to a square, the useful signal and noise can be sufficiently separated [11], [20]. So, we select positive integers n and m, $1 < n < N, m \geq 2, n \geq 2, m + n - 1 = N$, and n close to m; if N is even, $m = N/2, n = N/2 + 1$; if N is odd, $m = (N+1)/2, n = (N+1)/2$.

Singular value decomposition is an orthogonal transformation that could transform the original matrix into a diagonal matrix whose eigenvalues reflect some of the main features of the original matrix [16]. It will display different relationships among variables in a preferable way by altering the correlated variables to a group of uncorrelated ones [15]. By applying SVD, the matrix H can be decomposed into a product of three matrices and can be expressed as equation (2):

$$H = U \sum V^T \tag{2}$$

where T is the conjugate transpose, U and V are unitary matrices, $U = (u_1, u_2, \cdots, u_m)\,, u_i \in R^{m\times 1}$ and $V = (v_1, v_2, \cdots, v_n)\,, v_i \in R^{n\times 1}$, $\sum$ denotes non-negative diagonal matrix, $\sum = \begin{bmatrix} S & 0 \\ 0 & 0 \end{bmatrix}$ and $\mathrm{S} = \mathrm{diag}\,(\sigma_1, \sigma_2, \cdots, \sigma_r)$ with $\sigma_1 \geq \sigma_2 \geq \cdots \geq \sigma_r > 0$. $\sigma_1, \sigma_2, \cdots, \sigma_r$, and $\sigma_{r+1} = \sigma_{r+2} = \cdots = \sigma_n = 0$ are the positive square roots of the eigenvalues of $H^T H$ which are also called the singular values of H. The columns of U are called the left singular vectors of H, while the columns of V are called the right singular vectors of H. Singular values can reflect the major characteristic information of the raw signal. The larger the singular values, the more information it contains. The smaller the singular value, the less information. The singular value of noise is generally small. Thereby, the signal can be de-noised by selecting the appropriate singular values and the main information of the signal can be retained. A new matrix H' can be obtained by selecting the appropriate nonzero singular values for reconstruction.

$$H' = \sum_{i=1}^{k} \sigma_i u_i v_i^T \tag{3}$$

where k is the number of selected nonzero singular values, and the key to the reconstruction of matrix H' is how to determine k. If k is not properly selected, some useful information of the original signal will be lost, and it may even result in signal distortion after noise reduction. Therefore,

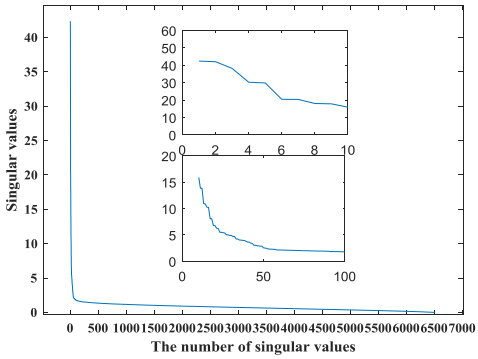

FIGURE 1. Singular values sequence of signal.

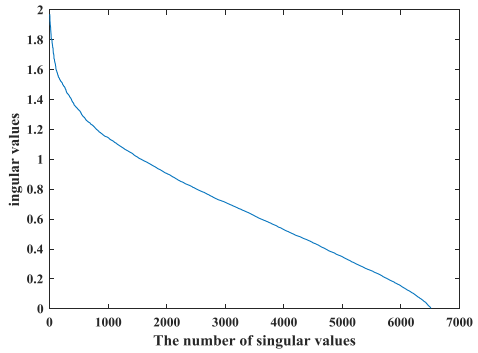

FIGURE 2. Singular values sequence of noise.

the key to realizing signal noise reduction with SVD is to select the singular values of the reconstructed signal using an appropriate threshold value.

B. SINGULAR VALUE THRESHOLD DETERMINATION

To keep the useful information and reduce the noise, we need to find a threshold point that can be used to distinguish the useful signal and noise. According to the literature [21], the singular values of the main signal are different from the singular values of the noise, so the mutation point of the slope of the singular value curve is the threshold point required. Some scholars take slope variation as a criterion for judging the threshold, but there may be points where the slope change is greatest before the correct threshold. Therefore, the threshold value obtained is not accurate. In this paper, we propose a new approach based on fitting to approximate the threshold point.

Figure 1 presents the sequence of singular values of the signal with a depth 3mm defect. We can know from the figure that the singular values appear in pairs, that is, adjacent singular values are close in size. We also know that the sequence of singular values consists of two curves with distinctly different slopes. Figure 2 shows the sequence of singular values of noise. The noise is a white Gaussian noise constructed randomly. The magnitude and distribution of the singular value of noise are different from that of EMAT signal. Therefore, the noise can be reduced by selecting the appropriate singular values. The singular values sequence decreases rapidly at first and then decreases slowly at a certain point. This is the point where the slope changes and this is the threshold point that we need. We propose a threshold

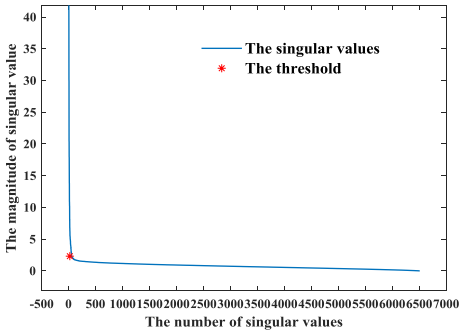

FIGURE 3. The fitting threshold.

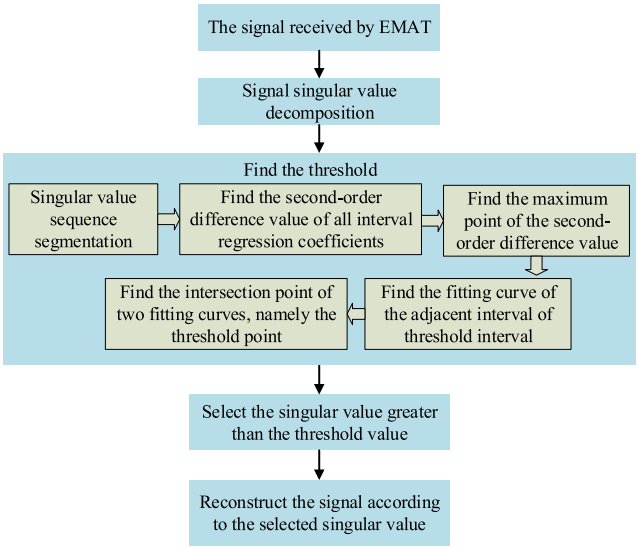

FIGURE 4. The flow chart of de-noising.

determination method based on the segmented regression model. The detailed steps are as follows:

Step1: Supposing that the singular value sequence of the raw signal is $\mathrm{SV} = (\mathrm{sv}_1, \mathrm{sv}_2, \mathrm{sv}_3, \cdots \mathrm{sv}_n)$. The $\boldsymbol{SV}$ is divided into $\boldsymbol{m}$ segments of the same length. Since the singular values appear in pairs, the number of data in each interval should be even.

Step2: Calculate the regression coefficient for each interval. The change point of the slope is not the point with the largest change of slope, but the point with the largest change rate of the slope. The interval of the slope change point is determined by the maximum of the second-order difference of the slope.

Step3: The data of two adjacent intervals of threshold interval is fitted using linear regression. The threshold is the intersection of two fitting curves. Figure 3 displays the threshold point we find.

The singular values larger than the threshold are selected to reconstruct the signal. The reconstructed signal is the signal after de-noising. The flow chart of de-noising is as follows:

III. EFFECTIVENESS ANALYSIS USING SIMULATION SIGNAL

This paper proposes an improved singular value decomposition de-noising approach based on the fitting threshold. The fitting threshold selection approach based on the

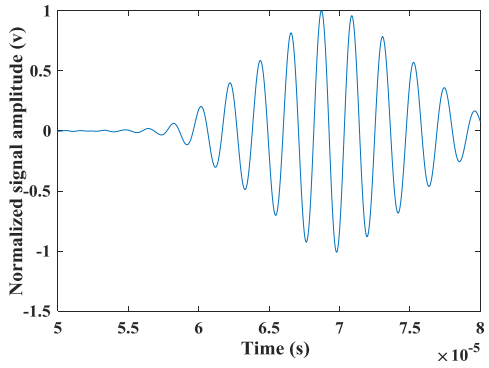

FIGURE 5. Simulation signal of Rayleigh wave in a sample with defect depth of 0 mm.

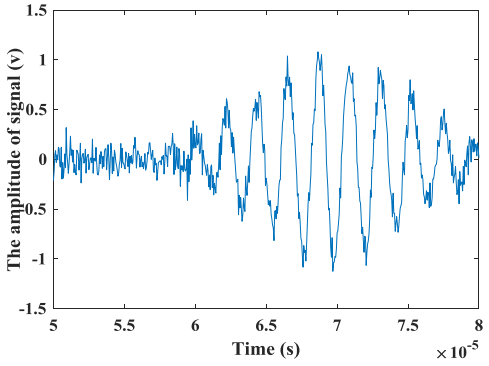

FIGURE 6. Simulation signal with random white Gaussian noise.

segmentation regression method can realize the adaptive threshold selection. We use the simulated Rayleigh wave signals with random Gaussian white noise to verify the effectiveness of the proposed method. The simulated signal of the Rayleigh wave is obtained by COMSOL Multi-physics [22]. Figure 5 displays the normalized simulated Rayleigh wave of a sample with no defect. Figure 6 presents the simulated signal with random Gaussian white noise.

In order to verify the pros and cons of the proposed approach, we use the three parameters of signal-to-noise ratio (SNR), root mean square error (RMSE), and waveform similarity coefficient (WSC) to evaluate the performance of noise reduction.

$$SNR = 10 \times \lg\left(\sum_{i=1}^{n} x^2(i) / \sum_{i=1}^{n} (x(i) - z(i))^2\right) \quad (4)$$

$$RMSE = \sqrt{1/n \times \left(\sum_{i=1}^{n} (z(i) - x\,(i))^2\right)} \quad (5)$$

$$WSC = \sum_{i=1}^{n} x\,(i) z\,(i) \Big/ \sqrt{\left(\sum_{i=1}^{n} x^2\,(i)\right)\left(\sum_{i=1}^{n} z^2\,(i)\right)} \quad (6)$$

In formula (4) (5) and (6), $x(i)$ denotes the original noise-free signal. $z(i)$ denotes the signal after noise reduction. The SNR reflects the quality of the signal after noise reduction. The higher the SNR is, the better the noise reduction effect will be. The RMSE represents the error between the signal after de-noising and the original signal. The larger the value is, the more information is lost after noise reduction, and the more serious the signal distortion is. The WSC describes the similarity in shape between the signal after de-noising and the original signal. The closer the WSC is to 1, the more similar it is to the original signal, and the smaller it is, the more serious the distortion is.

We will verify the effectiveness of the threshold selection method proposed in this paper comparing it with other threshold selection methods. Fig.7 (a) is the signal obtained by the SVD noise reduction method based on the fitting threshold proposed in this paper. The method filters out the added noise and gets a good consistency between the reconstructed signal and the original signal. Fig.7 (b) shows the signals after de-noising by SVD with different fixed thresholds. When the threshold is 3, the signal after noise reduction still contains a little noise. When the threshold value is 3.5, the noise reduction effect is similar to that when the threshold value is 4. However, compared with RMSE and WSC with the threshold value of 3.5 and 4 in Table 1, the noise reduction effect is better when the threshold value is 3.5. It reflects that the de-noising effect is different when the fixed threshold is different. Therefore, it is important to select a threshold for SVD-fixed threshold de-noising method, and the universality and operability of the fixed threshold are not strong.

Fig.7 (c) and Fig.7 (d) show the signals after de-noising using the singular value difference spectrum method and the singular value curvature spectrum method respectively. It is obvious that the signals obtained by these two methods have very serious distortion, so these two methods are not suitable for Rayleigh wave signal de-noising.

We also apply wavelet de-noising to process the noisy signal for comparison. Fig.7 (e) displays the result of wavelet de-noising. Most of the noise is filtered out, but the signal is slightly distorted. In comparison, the SVD de-noising method based on the fitting threshold is more suitable for Rayleigh wave signal de-noising.

IV. APPLICATION CASE ANALYSIS

In the practical application of electromagnetic ultrasonic transducer detection and evaluation of defects, signal preprocessing is an essential step. EMAT signal is vulnerable to noise, and the signal attenuates with the increase of defect depth, which makes EMAT signal noise reduction challenging. In this paper, we propose an improved SVD de-noising method based on the fitting threshold for EMAT signal. At the same time, we use experimental signals with different defect depths and different lift-off distances to verity the effectiveness of the proposed noise reduction method in this section. Furthermore, we characterize the depth of defect by the de-noised signal based on the lift-off slope.

A. EXPERIMENT DETAILS

The experimental platform of EMAT is the same as that in reference [23], [24]. As shown in figure8, the platform consists of a signal generator, a RITEC's GA-2500A gated pulse amplifier, a BR640 wideband receiver, an EMAT

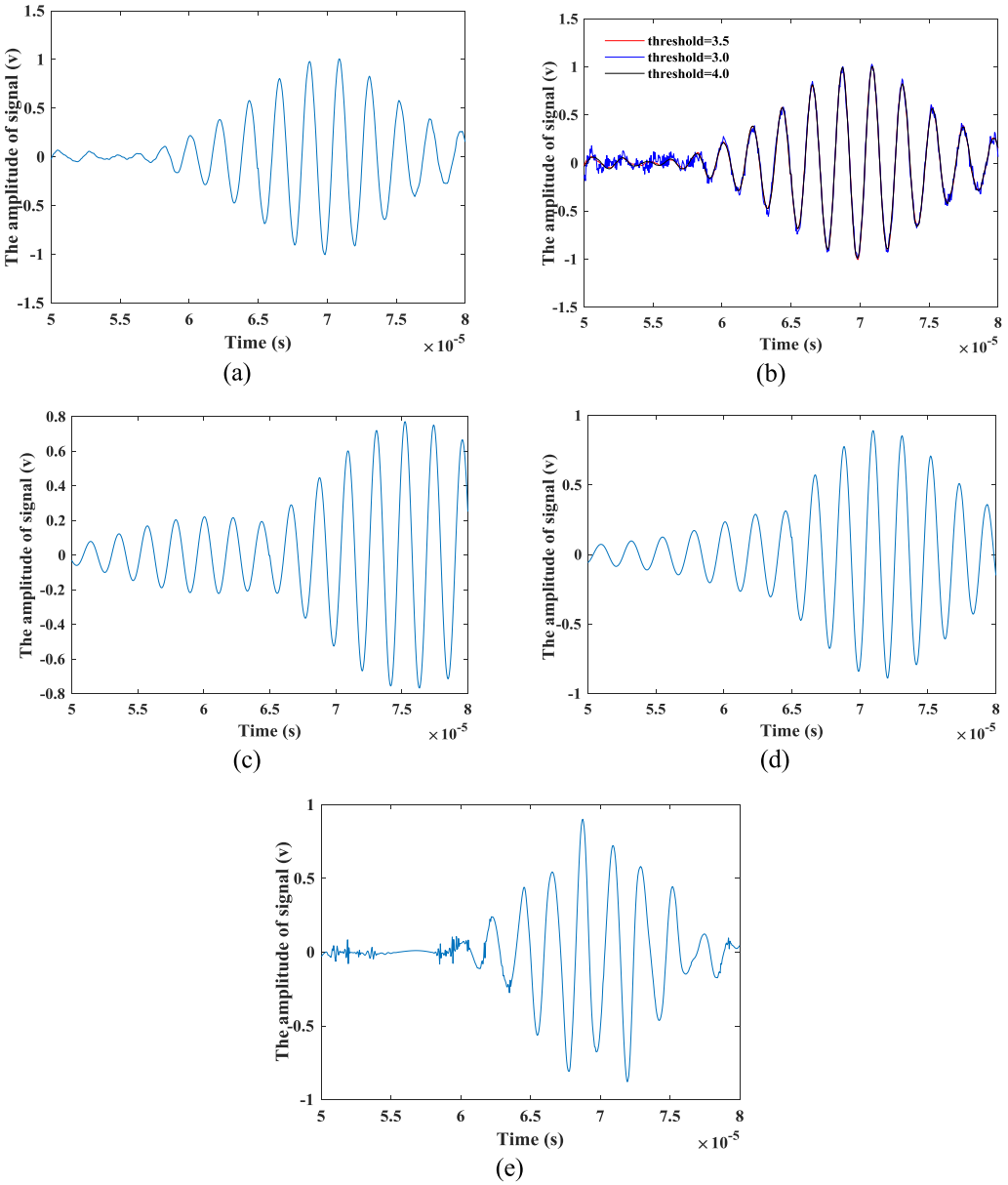

FIGURE 7. Signal after noise reduction by different de-noising methods. (a) SVD-fitting threshold. (b) SVD-fixed threshold. (c) SVD- singular value difference spectrum. (d) SVD- singular value curvature spectrum. (e) Wavelet de-noising.

TABLE 1. Results of different noise reduction methods.

Method \ Parameter		SNR	RMSE	WSC
The proposed approach		22.2059	0.1028	0.9970
SVD-fixed threshold	Th=3.0	17.6434	0.4012	0.9914
	Th=3.5	22.2059	0.1028	0.9970
	Th=4.0	22.3138	0.3986	0.9961
Singular value difference spectrum		4.7721	0.3342	0.8166
Singular value curvature spectrum		7.8378	0.3656	0.9140
The wavelet de-noising method		9.0326	0.1683	0.9576

transmitting probe T, an EMAT receiving probe R, an oscilloscope, and aluminum plates. The RITEC's GA-2500A gated pulse amplifier is used to amplify the sinusoidal pulses generated by the signal generator. Secondly, the high-power

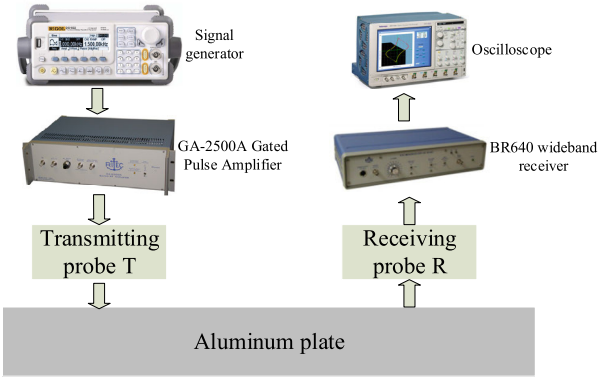

FIGURE 8. Schematic diagram of experimental system.

pulse current emitted is transmitted through the transmitting probe T, and the excited Rayleigh wave propagates

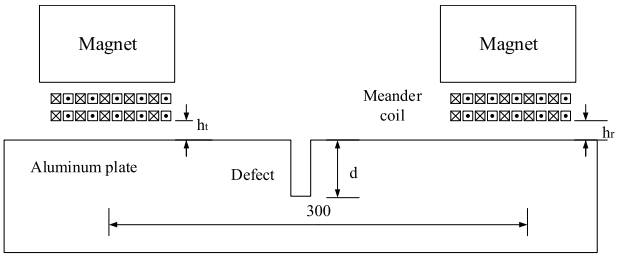

FIGURE 9. Schematic diagram of probe position.

in the sample and interacts with the defect. The receiving probe R receives signals from the aluminum plate. Finally, the received signal is then filtered and amplified by the BR640 wideband receiver and the processed data is saved and displayed on the oscilloscope.

The transmitting probe T and the receiving probe R are located at different sides of the defect, and the distance between them is 300mm as shown in Figure 9. The receiving probe R has the same structure as the transmitting probe T, which includes a permanent magnet and meander coil. The magnet size in the probe is 40 × 40 × 40 mm, providing a residual magnetic flux strength of 1.21T. The meander coil in the probe transmits a three-cycle sinusoidal pulse signal, and the excitation signal has a peak-to-peak voltage of 350V and a frequency of 500KHz. Since the single layer signal is weak, a double layer coil is used to increase the signal strength. Each layer has 10 coils, and each coil has 6 wires. The width of the wire is 0.15 mm, the height is 0.035 mm, and the length is 45mm. The spacing between the adjacent wires is 0.3 mm. The interval between the adjacent coils is 3.0 mm. In the figure 9, h_t represents the lifting distance of the transmitting probe, which remains unchanged at 0mm in the experiment. h_r is the lifting distance of the receiving probe, which varies from 0mm to 2mm.

The sample size is 500 * 250 * 60 mm and the material is 6061 aluminum alloy. At the center of the sample, the grooves were machined vertically on the surface with a width of 1 mm and depths of 0.5 mm, 1 mm, 1.3 mm, 2mm, 3 mm, 4mm, and 5 mm, respectively.

B. RESULT ANALYSIS

To verify the validity of the proposed method in practical application, we collected transmitted wave signals with different defects at different lift distances. We use the proposed SVD noise reduction method based on the fitting threshold to preprocess the experimental signal. In comparison, many different noise reduction methods are employed to conduct the de-noising process of experimental signal. Since the amount of noise contained in the experimental signal cannot be determined, the signal-to-noise ratio cannot be calculated. We use the ratio of the power of the original signal to the power of the filtered noise to express the performance of de-noising. The formula is as follows

$$SFN = 10 \times \lg\left(\sum_{i=1}^{n} x^2(i) / \sum_{i=1}^{n} (x(i) - z(i))^2\right) \quad (7)$$

TABLE 2. Results of different improved SVD noise reduction methods for experimental signals.

Defect depth d(mm)	Lift-off h_r (mm)	SVD-Fitting threshold		SVD-Fixed threshold		SVD-difference spectrum		SVD-curvature spectrum	
		SFR	WSC	SFR	WSC	SFR	WSC	SFR	WSC
0	0.1	22.5809	0.9973	32.5661	0.9997	3.0599	0.7157	2.2229	0.6391
0	1.0	29.8975	0.9995	25.6082	0.9987	3.1466	0.7407	1.5574	0.5903
0.5	0.1	28.0042	0.9992	33.1731	0.9998	2.2744	0.6462	1.1570	0.6462
0.5	1.0	26.2334	0.9989	25.2396	0.9986	8.9461	0.9402	1.7247	0.6229
1.0	0.1	23.8124	0.9980	31.9856	0.9997	1.9194	0.6002	2.5830	0.6781
1.0	1.0	25.7525	0.9988	25.5498	0.9988	2.1024	0.6761	0.7753	0.5128
1.3	0.1	26.1807	0.9988	29.9322	0.9995	1.9414	0.6120	1.9414	0.6120
1.3	1.0	20.9604	0.9964	24.1554	0.9983	8.4830	0.9334	1.4213	0.5874
2.0	0.1	13.5394	0.9796	23.9671	0.9982	1.6356	0.6111	1.6356	0.6111
2.0	1.0	16.1734	0.9919	15.3727	0.9902	0.6459	0.6497	0.6918	0.6565
3.0	0.1	18.2574	0.9930	21.2971	0.9965	1.6127	0.5927	1.6127	0.5927
3.0	1.0	16.6637	0.9896	15.9803	0.9878	4.0854	0.7913	1.1227	0.5104
4.0	0.1	28.2763	0.9993	31.1259	0.9996	2.2430	0.6458	2.2430	0.6458
4.0	1.0	14.5374	0.9923	14.4302	0.9921	1.1701	0.8153	2.4637	0.8667
5.0	0.1	10.8825	0.9634	18.6161	0.9939	1.3459	0.5947	1.0538	0.5538
5.0	1.0	11.2044	0.9675	11.7503	0.9714	0.1492	0.4299	0.5227	0.5020

This formula (7) is the same as the SNR formula, but the meaning is different, which is the ratio of the power of the original signal to the power of the filtered noise. $x(i)$ denotes the original noisy transmitted wave signal. $z(i)$ denotes the signal after noise reduction. $x(i) - z(i)$ represents the signal filtered out by the filtering process, rather than all the noise contained in the signal. The greater the difference, the more noise is filtered out. Thus, the smaller the value of *SFN*, the more noise will be filtered out. However, if the value *SFN* is too small, the signal will be severely distorted. The WSC describes the difference in shape between the de-noised signal and the original signal, which can be used to evaluate the distortion of the signal. The smaller the WSC, the greater the distortion.

To verify the effectiveness of the SVD de-noising method based on fitting threshold proposed in this paper, we compare it with different improved SVD de-noising methods. Table 2 lists the de-noising results of different improved SVD de-noising methods for signals with different defect depths and different lift-off distances. It can be seen from the table that the SFN of SVD-fitting threshold method is less than the SFN of SVD-fixed threshold, and the WSC of the two are equivalent. Additionally, the SVD de-noising based on fitting threshold can adaptively obtain the appropriate threshold for different signals. Thus, the SVD-fitting threshold

TABLE 3. Results of different latest noise reduction methods for experimental signals.

Defect depth d(mm)	Lift-off h_r (mm)	VMD		Wavelet		Wavelet packet-SVD		EMD-wavelet	
		SFR	WSC	SFR		SFR		SFR	WSC
0	0.1	4.5556	0.9786	37.0945	0.9999	53.2543	1.0000	15.7726	0.9869
0	1.0	3.7093	0.9452	37.4844	0.9999	44.6138	1.0000	9.8255	0.9502
0.5	0.1	4.3390	0.9798	41.6702	0.9999	55.3597	1.0000	13.1039	0.9757
0.5	1.0	3.2474	0.9302	39.0579	0.9999	45.8647	1.0000	8.1149	0.9271
1.0	0.1	4.2803	0.9779	42.0074	0.9999	54.8832	1.0000	12.0851	0.9693
1.0	1.0	2.9246	0.9151	39.6992	0.9999	46.5532	1.0000	7.1599	0.9115
1.3	0.1	4.2236	0.9758	39.9915	0.9999	53.2980	1.0000	13.4310	0.9776
1.3	1.0	3.1941	0.9279	38.7505	0.9999	44.8966	1.0000	7.9526	0.9246
2.0	0.1	3.6858	0.9040	29.8419	0.9995	44.2700	1.0000	6.5824	0.8955
2.0	1.0	0.3828	0.7268	28.3470	0.9995	34.8570	0.9999	1.0351	0.7252
3.0	0.1	3.7495	0.9306	31.1515	0.9996	45.4205	1.0000	8.2469	0.9276
3.0	1.0	3.7268	0.9220	30.9555	0.9996	39.4603	0.9999	9.3042	0.9421
4.0	0.1	4.2470	0.9764	41.0982	0.9999	52.8808	1.0000	10.7252	0.9579
4.0	1.0	2.4765	0.5504	29.1639	0.9997	36.1833	0.9999	2.2533	0.5196
5.0	0.1	3.5924	0.8589	27.0345	0.9991	45.6120	1.0000	6.4009	0.8942
5.0	1.0	2.0725	0.7536	26.2804	0.9990	36.6590	0.9999	3.1649	0.8620

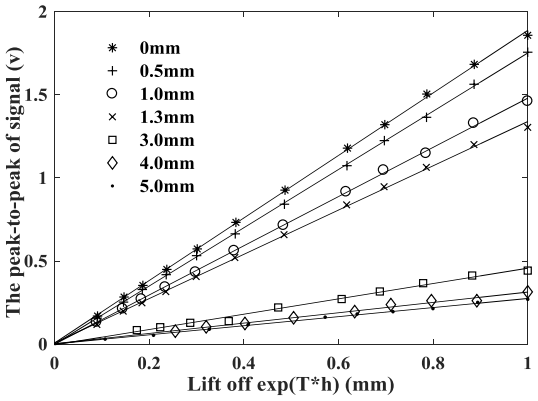

FIGURE 10. Normalized lift off slope.

de-noising method is superior to the SVD- fixed threshold method for EMAT signals. The WSC of SVD-difference spectrum method and SVD-curvature spectrum method are between 0.5 and 0.9, indicating that the signals after noise reduction have great distortion. Therefore, the improved SVD de-noising method based on fitting threshold has been verified to be effective for noise reduction of EMAT signals.

We also verify the effectiveness of the proposed method by comparing it with other state of-the art de-noising methods on the EMAT signal [14], [25]–[27]. Table 3 shows the results

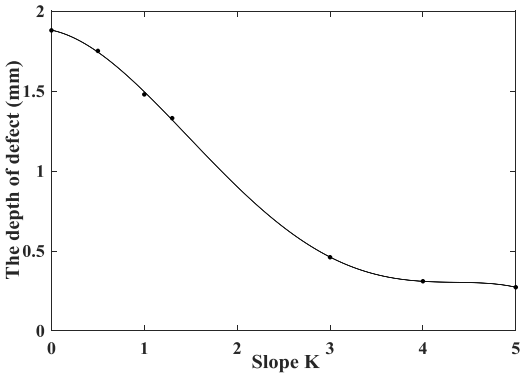

FIGURE 11. Lift-off slope fitting curve.

TABLE 4. The calculation depth and relative error of the characterization after different noise reduction.

Defect depth d(mm)	SVD-Fitting threshold		Wavelet de-noising		SVD-Fixed threshold		SVD-difference spectrum	
	Calculated depth (mm)	Relative Error	Calculated depth (mm)	Relative Error	Calculated depth (mm)	Relative Error	Calculated depth (mm)	Relative Error
0	0.0123	/	0.0143	/	0.0205	/	0.0840	/
0.5	0.4812	3.76%	0.4703	5.94%	0.4709	5.82%	0.5489	9.78%
1.0	1.0292	2.92%	1.0470	4.70%	1.0443	4.43%	0.9136	8.64%
1.3	1.2813	1.44%	1.2698	2.32%	1.2716	2.18%	1.3511	6.64%
3.0	3.0040	0.13%	3.0061	0.20%	3.0060	0.20%	2.9922	0.26%
4.0	3.9857	0.36%	3.9776	0.56%	3.9799	0.50%	4.0165	0.41%
5.0	5.0007	0.01%	5.0011	0.02%	5.0010	0.02%	4.9995	0.01%

Defect depth d(mm)	SVD-curvature spectrum		Wavelet packet-SVD		EMD-wavelet		VMD	
	Calculated depth (mm)	Relative Error	Calculated depth (mm)	Relative Error	Calculated depth (mm)	Relative Error	Calculated depth (mm)	Relative Error
0	0.0674	/	0.0560	/	0.1874	/	0.0017	/
0.5	0.5128	2.56%	0.4910	1.8%	0.4501	9.98%	0.5454	9.08%
1.0	0.9808	1.92%	1.0443	4.43%	0.9102	8.98%	1.0155	1.55%
1.3	1.3121	0.93%	1.2595	3.12%	1.1660	10.31%	1.2456	4.18%
3.0	2.9980	0.06%	3.0232	0.77%	3.3170	10.57%	3.0661	2.20%
4.0	4.2681	6.70%	3.9414	1.47%	3.7444	6.39%	3.8821	2.95%
5.0	4.5601	8.80%	5.0067	0.13%	4.9398	1.20%	5.0321	0.64%

of different latest noise reduction methods. We can know that signals with crack depth greater than 2 mm at 1mm lift-off distance are distorted after noise reduction by the variational mode decomposition (VMD) de-noising method and EMD-wavelet de-noising method. From the Table 3, it is apparent that the SFR of wavelet de-noising and wavelet packet-SVD de-noising method are greater than that of the

proposed method, and the WSC of both methods are greater than 0.99, indicating that these two methods filter out very little noise. Thereby, the improved SVD de-noising method based on fitting threshold is more suitable for EMAT signal than other latest methods.

In reference [24], Zhang Kang proposed a characterization method of surface defect based on the lift-off slope. There is a linear relationship between the exponential form of lift off distance ($exp(T^*hr)$) and signal strength (v_{pp}) as shown in figure 10. The slope K is different when the depth of defect is different, and the slope K decreases monotonically when the depth of defect increases in figure 11. In this paper, we use the lift-off slope to evaluate the defect quantitatively. After noise reduction using different methods, the calculated depths of defects and relative errors are listed in Table 4. We can know that the relative error of defect characterization is the smallest after noise reduction using the SVD-fitting threshold method, which is less than 4%. It is obvious that after noise reduction using SVD-difference spectrum, SVD-curvature spectrum, EMD-wavelet, and VMD de-noising respectively, the relative errors of defect characterization are very larger, which are all greater than 8%. According to the analysis of results in Table 4, the maximum relative errors of the proposed method are reduced by 36.70%, 35.40%, 61.55%, 57.27%, 15.12%, 62.59, and 58.59%, respectively compared with those of different methods. Therefore, the SVD noise reduction method based on the fitting threshold is beneficial to improve the quantification accuracy of defect depth.

V. CONCLUSION

To develop a more reasonable and practical de-noising method for the EMAT signal, a fitting threshold is proposed for improving the SVD noise reduction method in this paper. With the aid of fitting threshold, the effective singular value order of the SVD noise reduction method is determined. The effectiveness of this method is verified by simulation signals and experimental signals. From the calculation results and discussion, the following conclusions can be drawn.

(1) Aiming at the distribution characteristics of singular values of electromagnetic ultrasonic signals, a fitting threshold method based on a segmented regression model is proposed to obtain the effective singular value order. This method can adaptively determine the selection of singular values.

(2) The effectiveness of the proposed method is analyzed by simulation signals and experimental signals. The method in this paper can achieve fairly better noise reduction effect for EMAT signal compared with other methods.

(3) After noise reduction of the experimental signal by different methods, we obtained the defect depth based on the lift-off slope. The results show that the SVD noise reduction method based on fitting threshold can obtain more accurate characterization results, and the relative error of characterization is the smallest compared with other methods.

ACKNOWLEDGMENT

The authors would like to thank Mr. K Zhang for his contribution in this article.

REFERENCES

[1] S. Dixon, S. E. Burrows, B. Dutton, and Y. Fan, "Detection of cracks in metal sheets using pulsed laser generated ultrasound and EMAT detection," *Ultrasonics*, vol. 51, no. 1, pp. 7–16, Jan. 2011, doi: 10.1016/j.ultras.2010.05.002.

[2] A. Sophian, G. Y. Tian, and S. Zairi, "Pulsed magnetic flux leakage techniques for crack detection and characterisation," *Sens. Actuators A, Phys.*, vol. 125, no. 2, pp. 186–191, Jan. 2006, doi: 10.1016/j.sna.2005.07.013.

[3] B. Lei, P. Yi, Y. Li, and J. Xiang, "A temperature drift compensation method for pulsed eddy current technology," *Sensors*, vol. 18, no. 6, p. 1952, Jun. 2018, doi: 10.3390/s18061952.

[4] S. E. Burrows, Y. Fan, and S. Dixon, "High temperature thickness measurements of stainless steel and low carbon steel using electromagnetic acoustic transducers," *NDT E Int.*, vol. 68, pp. 73–77, Dec. 2014, doi: 10.1016/j.ndteint.2014.07.009.

[5] R. Benegal, F. Karimi, T. Filleter, and A. N. Sinclair, "Optimization of periodic permanent magnet configuration in lorentz-force EMATs," *Res. Nondestruct. Eval.*, vol. 29, no. 2, pp. 95–108, Apr. 2018, doi: 10.1080/09349847.2016.1262485.

[6] S. Huang, W. Zhao, Y. Zhang, and S. Wang, "Study on the lift-off effect of EMAT," *Sens. Actuators A, Phys.*, vol. 153, no. 2, pp. 218–221, Aug. 2009, doi: 10.1016/j.sna.2009.05.014.

[7] X. Wen, G. Lu, J. Liu, and P. Yan, "Graph modeling of singular values for early fault detection and diagnosis of rolling element bearings," *Mech. Syst. Signal Process.*, vol. 145, Nov. 2020, Art. no. 106956, doi: 10.1016/j.ymssp.2020.106956.

[8] X. Xu, M. Luo, Z. Tan, and R. Pei, "Echo signal extraction method of laser radar based on improved singular value decomposition and wavelet threshold denoising," *Infr. Phys. Technol.*, vol. 92, pp. 327–335, Aug. 2018, doi: 10.1016/j.infrared.2018.06.028.

[9] M. Z. Silva, R. Gouyon, and F. Lepoutre, "Hidden corrosion detection in aircraft aluminum structures using laser ultrasonics and wavelet transform signal analysis," *Ultrasonics*, vol. 41, no. 4, pp. 301–305, 2003, doi: 10.1016/s0041-624x(02)00455-9.

[10] Y. Yu, H. Zhang, and V. Singh, "Forward prediction of runoff data in data-scarce basins with an improved ensemble empirical mode decomposition (EEMD) model," *Water*, vol. 10, no. 4, p. 388, Mar. 2018, doi: 10.3390/w10040388.

[11] J. C. Lazaro, "Noise reduction in ultrasonic NDT using discrete wavelet transform processing," in *Proc. IEEE Ultrason. Symp.*, vol. 1, 2002, pp. 777–780, doi: 10.1109/ULTSYM.2002.1193514.

[12] E. Pardo, J. L. San Emeterio, M. A. Rodriguez, and A. Ramos, "Noise reduction in ultrasonic NDT using undecimated wavelet transforms," *Ultrasonics*, vol. 44, pp. e1063–e1067, Dec. 2006, doi: 10.1016/j.ultras.2006.05.101.

[13] S. P. Song and P. W. Que, "Wavelet based noise suppression technique and its application to ultrasonic flaw detection," *Ultrasonics*, vol. 44, pp. 93–188, Feb. 2006, doi: 10.1016/j.ultras.2005.10.004.

[14] H. Li, T. Liu, X. Wu, and Q. Chen, "Research on bearing fault feature extraction based on singular value decomposition and optimized frequency band entropy," *Mech. Syst. Signal Process.*, vol. 118, pp. 477–502, Mar. 2019, doi: 10.1016/j.ymssp.2018.08.056.

[15] L. Rong and P. Shang, "New irreversibility measure and complexity analysis based on singular value decomposition," *Phys. A, Stat. Mech. Appl.*, vol. 512, pp. 913–924, Dec. 2018, doi: 10.1016/j.physa.2018.08.097.

[16] G. Zhang, B. Xu, K. Zhang, J. Hou, T. Xie, X. Li, and F. Liu, "Research on a noise reduction method based on multi-resolution singular value decomposition," *Appl. Sci.-Basel*, vol. 10, p. 17, Feb. 2020, doi: 10.3390/app10041409.

[17] W.-X. Yang and P. W. Tse, "Development of an advanced noise reduction method for vibration analysis based on singular value decomposition," *NDT&E Int.*, vol. 36, no. 6, pp. 419–432, 2003, doi: 10.1016/s0963-8695(03)00044-6.

[18] Y. Zhicheng, L. Bin, and C. Lianping, "Calibration of tri-axis magnetometers using an improved truncated singular value decomposition method," *Meas. Sci. Technol.*, vol. 29, no. 12, Dec. 2018, Art. no. 125101, doi: 10.1088/1361-6501/aae16d.

[19] X. Zhao and B. Ye, "Selection of effective singular values using difference spectrum and its application to fault diagnosis of headstock," *Mech. Syst. Signal Process.*, vol. 25, no. 5, pp. 1617–1631, Jul. 2011, doi: 10.1016/j.ymssp.2011.01.003.
[20] B. Muruganatham, M. A. Sanjith, B. Krishnakumar, and S. A. V. S. Murty, "Roller element bearing fault diagnosis using singular spectrum analysis," *Mech. Syst. Signal Process.*, vol. 35, nos. 1–2, pp. 150–166, Feb. 2013, doi: 10.1016/j.ymssp.2012.08.019.
[21] X. Zhao, B. Ye, and T. Chen, "Extraction method of faint fault feature based on wavelet-SVD difference spectrum," *Chin. J. Mech. Eng.*, vol. 48, no. 7, pp. 37–48, 2012.
[22] P. Yi, K. Zhang, Y. Li, and X. Zhang, "Influence of the lift-off effect on the cut-off frequency of the EMAT-generated Rayleigh wave signal," *Sensors*, vol. 14, pp. 19687–19699, Oct. 2014, doi: 10.3390/s141019687.
[23] B. Lei, P. Yi, and J. Xiang, "A new defect classification approach based on the fusion matrix of multi-eigenvalue," *IEEE Sensors J.*, vol. 21, no. 3, pp. 3398–3407, Feb. 2021, doi: 10.1109/jsen.2020.3024753.
[24] K. Zhang, P. Yi, Y. Li, B. Hui, and X. Zhang, "A new method to evaluate surface defects with an electromagnetic acoustic transducer," *Sensors*, vol. 15, pp. 17420–17432, Jul. 2015, doi: 10.3390/s150717420.
[25] D. Si, B. Gao, W. Guo, Y. Yan, G. Y. Tian, and Y. Yin, "Variational mode decomposition linked wavelet method for EMAT denoise with large lift-off effect," *NDT E Int.*, vol. 107, Oct. 2019, Art. no. 102149, doi: 10.1016/j.ndteint.2019.102149.
[26] Z. Nie, K. Wang, and M. Zhao, "Application of wavelet and EEMD joint denoising in nonlinear ultrasonic testing of concrete," *Adv. Mater. Sci. Eng.*, vol. 2018, pp. 1–11, Jan. 2018, doi: 10.1155/2018/7872036.
[27] J. Zhang, Q. Jiang, B. Ma, Y. Zhao, and L. Zhu, "Signal de-noising method for vibration signal of flood discharge structure based on combined wavelet and EMD," *J. Vib. Control*, vol. 23, no. 15, pp. 2401–2417, Aug. 2017, doi: 10.1177/1077546315616551.

BITING LEI was born in Shaanxi, China, in 1992. She received the B.S. degree in mechatronic engineering from Chang'an University, Xi'an, China, in 2016. She is currently pursuing the Ph.D. degree in mechanical engineering with the Huazhong University of Science and Technology, Wuhan, China. Her research interest includes electromagnetic nondestructive testing.

PENGXING YI (Member, IEEE) was born in Changde, China, in 1974. He received the B.S. degree in mechatronic engineering from the Wuhan University of Science and Technology, Wuhan, China, in 1997, and the M.S. and Ph.D. degrees in mechanical engineering from the Huazhong University of Science and Technology, Wuhan, in 2003 and 2007, respectively. From 2007 to 2009, he was a Postdoctoral Research Fellow with the Department of Control Science and Engineering, Huazhong University of Science and Technology, where he has been an Associate Professor with the School of Mechanical Science and Engineering, since 2009. From 2013 to 2014, he was a Visiting Professor with the Georgia Institute of Technology, Atlanta, GA, USA. His research interests include NDT, high speed data acquisition and signal processing, and intelligent monitoring methods in manufacturing.

JIAYUN XIANG was born in Jiangxi, China, in 1995. He received the B.S. degree in mechanical and transportation engineering from Hunan University. He is currently pursuing the master's degree in mechanical engineering with the Huazhong University of Science and Technology, Wuhan, China. His primary research interest includes electromagnetic nondestructive testing. His awards and honors include the National Scholarship of China and the National Inspirational Scholarship of China.

WEI XU was born in Chongqing, in 1995. He received the bachelor's degree in mechanics from Shihezi University. He is currently pursuing the master's degree in mechanical engineering with the Huazhong University of Science and Technology.

His main research interests include electromagnetic nondestructive testing and weak electrical signal detection.